Chemical stability of a cold-active cellulase with high tolerance toward surfactants and chaotropic agent

Thaís V. Souza[a,1], Juscemácia N. Araujo[a,1], Viviam M. da Silva[a], Marcelo V. Liberato[b], Agnes C. Pimentel[b], Thabata M. Alvarez[b], Fabio M. Squina[b], Wanius Garcia[a,*]

[a] Centro de Ciências Naturais e Humanas, Universidade Federal do ABC (UFABC), Santo André, SP, Brazil
[b] Laboratório Nacional de Ciência e Tecnologia do Bioetanol (CTBE), Centro Nacional de Pesquisa em Energia e Materiais (CNPEM), Campinas, SP, Brazil

ARTICLE INFO

ABSTRACT

CelE1 is a cold-active endo-acting glucanase with high activity at a broad temperature range and under alkaline conditions. Here, we examined the effects of pH on the secondary and tertiary structures, net charge, and activity of CelE1. Although variation in pH showed a small effect in the enzyme structure, the activity was highly influenced at acidic conditions, while reached the optimum activity at pH 8. Furthermore, to estimate whether CelE1 could be used as detergent additives, CelE1 activity was evaluated in the presence of surfactants. Ionic and nonionic surfactants were not able to reduce CelE1 activity significantly. Therefore, CelE1 was found to be promising candidate for use as detergent additives. Finally, we reported a thermodynamic analysis based on the structural stability and the chemical unfolding/refolding process of CelE1. The results indicated that the chemical unfolding proceeds as a reversible two-state process. These data can be useful for biotechnological applications.

© 2015 The Authors. Published by Elsevier B.V. This is an open access article under the CC BY-NC-ND license (http://creativecommons.org/licenses/by-nc-nd/4.0/).

1. Introduction

Cellulose is the most abundant polysaccharide found in the cell walls of plants, and provides the major renewable energy source on the planet [1,2]. Cellulases are important enzymes produced by various groups of microorganisms that can hydrolyze the β-1,4-linkage between the glucose units of the cellulose polymer. These enzymes are classified into glycoside hydrolase (GH) families and can be divided into three groups: endoglucanases (EC 3.2.1.4), cellobiohydrolases (EC 3.2.1.91), and β-glucosidases (EC 3.2.1.21) [3].

The complete enzymatic hydrolysis of cellulose polymers to glucose units requires at least one type of each enzyme described above working synergistically [4–6]. Briefly, endoglucanases randomly cleave the β-1,4-glycosidic linkages of cellulose, while cellobiohydrolases cleave off cellobiose units (dimer of glucose) from the reducing or nonreducing end of cellulose chain [4,5]. At last, β-glucosidases hydrolyze the released cellobiose to glucose [6,7].

A recent study reported a novel cellulase identified from a sugarcane soil metagomic library [8]. This cellulase named CelE1,

belonging to GH5 family, showed unusual catalytic properties. CelE1 is an endo-acting glucanase with high catalytic activity at a broad temperature range. Furthermore, CelE1 showed high catalytic activity at alkaline pH values, conditions that commonly cause enzyme inactivation of classical acidic cellulases [8]. Also, CelE1 is a cold-active enzyme that retains more than 70% of the activity at temperatures between 10 °C and 50 °C [8].

Cellulases are being used in several industrial applications, for example, in the pulp and paper, textile, and detergent industries, and more recently in the field of plant structural polysaccharides conversion into bioenergy [9–11]. Specifically, as essential criteria for using of cellulases as detergent additives, the enzyme should be active under low temperature, stable under alkaline conditions, and compatible with detergents [11]. Alkaline cellulases are added into detergents for laundry purposes. For example, cellulases remove cellulose microfibrils produced during manufacturing and washing of the cotton-based cloth [9]. The detergent industry has interest on cellulases for lower washing temperatures and also reduction in water consumption [12].

In this study, we examined the effects of pH on the secondary and tertiary structures, net charge, and also enzymatic activity of CelE1 using biophysical and biochemical techniques. Furthermore, to estimate whether CelE1 could be used as detergent additives, CelE1 activity was evaluated in the presence of surfactants (ionic and nonionic). Finally, we reported a thermodynamic analysis based on the structural stability and the chemical unfolding/

---

* *Corresponding author.
E-mail address: wanius.garcia@ufabc.edu.br (W. Garcia).
[1] These authors contributed equally to this work.

refolding process of the recombinant CelE1. These studies are very important to understand the relationship among CelE1 structure, stability, and activity. Also, the data reported here can be useful for biotechnological applications, especially in detergent industries.

2. Materials and methods

2.1. Materials

LB medium, isopropyl-β-D-thiogalactopyranoside (IPTG), nickel-nitrilotriacetic acid resin (Ni-NTA), imidazole, carboxymethyl cellulose (CMC), kanamycin, urea, Triton X-100, sodium dodecyl sulfate (SDS), protein standards used as SDS-polyacrylamide gel electrophoresis (SDS-PAGE) markers were purchased from Sigma. All chemicals and reagents used in this study were of the highest purity analytical grade.

2.2. Expression and purification of recombinant CelE1

The expression and purification of recombinant CelE1 was carried out as reported previously with minor modifications [8]. Briefly, 1L of LB medium containing kanamycin (50 μg/mL), inoculated with *Escherichia coli* BL21(DE3) containing the expression plasmid, was incubated at 37 °C in shake flasks until attaining an optical density of 0.5 at 600 nm. IPTG was added to a final concentration of 0.5 mM, and incubation continued at 37 °C for 4 h. After incubation, the cells were harvested by centrifugation at 5,000 × g for 20 min at 4 °C, resuspended in 20 mM acetate–borate–phosphate buffer adjusted at pH 7.4, and disrupted by sonication. The suspension was then centrifuged at 5,000 × g for 20 min at 4 °C to separate the cell debris. The supernatant containing the recombinant CelE1 was applied to a nickel-affinity column equilibrated with 20 mM acetate–borate–phosphate buffer adjusted at pH 7.4. CelE1 was eluted from the column with the same buffer containing 150 mM imidazole. The purity of the final CelE1 was verified by 15% SDS-PAGE. CelE1 was exhaustively dialyzed in 20 mM acetate–borate–phosphate buffer adjusted at pH 7.4 for elimination of imidazole. The concentration of recombinant CelE1 was determined by UV absorbance at 280 nm using a theoretical extinction coefficient ($\varepsilon_{280\,nm}$) based on the amino acid composition. The $\varepsilon_{280\,nm} = 85,370\,M^{-1}\,cm^{-1}$ was determined for the monomer using the ProtParam tool [13]. The final CelE1 was stored at 4 °C and used until four days after the purification.

2.3. Activity assay

Enzymatic activity assays were performed by a colorimetric method using the 3,5-dinitrosalicylic acid (DNS) [8,14] with glucose being a standard for the calibration curves. Assays of optimal pH were performed in triplicate with CMC as the substrate. The reaction mixture containing 50 μL of enzyme at 0.2 μM, 0.2% (w/v) CMC and 150 mM acetate/fosfate/glycine buffer was incubated at 25 °C for 10 min and stopped by adding 50 μL of DNS solution. After this, the mixture was incubated again for 5 min at 95 °C and the absorbance was measured at 540 nm. To assess the enzyme activity resistance to the presence of surfactants and urea, 0.2 μM enzyme was incubated with different concentrations of urea, SDS and Triton X-100 at different periods of time. Then, a reaction in the same setup for pH test was performed using 50 mM sodium phosphate buffer instead of acetate/phosphate/glycine buffer. The refolding experiment was carried out with the enzyme incubation with 7 M urea for 2 h, followed by dilutions in 50 mM sodium phosphate buffer. After a new incubation for 2 h, the activity was measured as previously described.

2.4. Dynamic light scattering (DLS)

The size characteristics of recombinant CelE1 was examined employed the Nano-ZS dynamic light scattering system (Malvern Instruments Ltd., Malvern, UK) [15]. This system uses a 633 nm laser and a fixed scattering angle (173°). Protein solutions (1 and 5 mg/mL), in 20 mM acetate–borate–phosphate buffer adjusted at pH 7, was first passed through a 0.22 μm filter (Millipore, USA), centrifuged at 16,000 × g for 10 min, and subsequently loaded into a quartz cuvette prior to measurement. The hydrodynamic radius (R_S) was determined from a second order cumulant fit to the intensity auto-correlation function (size distribution by volume). The determined R_S was converted to molecular mass (kilo-Daltons) on the basis of the assumption of a spherical particle and using the Zetasizer software.

2.5. Electrophoretic light scattering (ELS)

ELS measurements were employed to determine the average zeta-potential (ζ) of recombinant CelE1, which were collected using a Zetasiser nano-ZS at 25 °C [16]. Zeta-potential were measured for a fixed enzyme concentration of 1 mg/mL in 20 mM acetate–borate–phosphate buffer adjusted to the different pH values. This instrument measures the electrophoretic mobility (μ_e) and converts the value to a zeta-potential (mV) through Henry's equation [16]: $\mu_e = [2\varepsilon\zeta F(\kappa a)]/3\eta$, where ε is the dielectric constant of water and η is the viscosity. Furthermore, $F(\kappa a)$ is the Henry's function, which was calculated through the Smoluchowski approximation with $F(\kappa a) = 1.5$. The isoelectric point is given by the pH value at which the zeta-potential is approximately zero [16].

2.6. Far-UV circular dichroism (CD) spectroscopy

CD spectra were measured using a Jasco J-815 spectropolarimeter equipped with a temperature control device. CelE1 concentration was 8 μM in 20 mM acetate–borate–phosphate buffer adjusted to the different pH values. All data were measured at 25 °C using 0.1 cm quartz cuvette and the spectra were recorded over the wavelength range from 195 to 260 nm. Eight accumulations were averaged to form the CD spectra, using a scanning speed of 100 nm min^{-1}, a spectral bandwidth of 1 nm, and a response time of 0.5 s, and obtained on degree scale. Chemical unfolding was carried out by increasing the urea concentration from 0 to 7.5 M while monitoring the ellipticity change at 220 nm. CelE1 was incubated for 18 h in the corresponding buffer prior to measurements. All experiments were performed three times, and the buffer contribution was subtracted in all of the experiments. The fraction of denatured CelE1, α, was calculated from the equations [17]: $\alpha = \frac{(\theta_N - \theta_{obs})}{(\theta_N - \theta_D)}$ and $\alpha + \beta = 1$, in which θ_{obs} is the ellipticity obtained at a particular urea concentration, and θ_D and θ_N are the values of the ellipticity characteristic of the denatured and native states, respectively. Chemical unfolding data were fit using a two-state model [17,18].

2.7. Intrinsic fluorescence spectroscopy

Intrinsic fluorescence spectroscopy measurements were performed on a steady-state spectrofluorometer model Cary Eclypse Varian, equipped with a refrigerated circulator. The tryptophan residues of CelE1 were excited at 295 nm. Fluorescence emission spectra (averaged 5 times) were recorded in a 1 cm path length quartz cuvette from 300 to 450 nm. CelE1 concentration was 3 μM in 20 mM acetate–borate–phosphate buffer adjusted to the different pH values. Chemically unfolding curve was obtained by

increasing the urea concentration from 0 to 7.5 M and measuring the fluorescence intensity at 338 nm. The protein was incubated for 18 h in the corresponding buffer prior to measurements. All experiments were performed three times, and the buffer contribution was subtracted in all of the experiments. The fraction of denatured protein, α, was calculated from the equations [17]: $\alpha = \frac{(I_N - I_{obs})}{(I_N - I_D)}$ and $\alpha + \beta = 1$, in which I_{obs} is the fluorescence intensity obtained at a particular urea concentration, and I_D and I_N are the values of the fluorescence intensity characteristic of the denatured and native states, respectively. Chemical unfolding results were fit using a two-state model [17,18]. Refolding of CelE1 (at 7.5 M urea) was done by quick dilution (1:40 fold) against the same buffer without urea and under gentle agitation.

3. Results and discussion

3.1. Effect of pH at 25 °C on the enzymatic activity of CelE1

The production of CelE1 by heterologous expression methodology was successful, resulting in large amount of fully active enzyme (with unusual biochemical properties) for industrial processes. A recent paper reported that CelE1 possesses high activity at a broad temperature range and under alkaline conditions [8]. CelE1 was highly active against CMC and showed an optimum activity determined at 50 °C and pH 7 [8]. In order to compare the structural stability with its function, CelE1 activity was studied at 25 °C as a function of pH. As determined previously, CelE1 is active in a broad range of pH (Fig. 1A). However, at 25 °C, the activity in low pH, such as 5 and 6, was reduced when

compared to the activity at 37 °C [8]. The enzyme reached its optimum activity at pH 8, while at pH 4 the remaining activity was virtually zero. Unusually, the enzyme keeps 43% of activity at pH 10 (Fig. 1A).

3.2. Reversible unfolding of CelE1

CelE1 activity was also evaluated in the presence of chaotropic agent (urea) at 25 °C (Fig. 1B). The enzymatic activity of CelE1 decreases with the increase in urea concentration. The incubation with 3 M urea during 1 h (or 15 h) was enough to reduce the activity to 70%. The enzyme still showed around 15% of activity when incubated with 7 M urea during 15 h, and it was completely inactivated when incubated with 7 M urea during periods longer than 15 h (data not shown). The refolding of CelE1, in the conditions described here, showed that the chemical denaturation by urea was a reversible process (Fig. 1C). Unfolded and subsequently refolded CelE1 maintains approximately 100% of its native activity in the conditions described in this study.

3.3. Evaluation of CelE1 activity in the presence of surfactants

The main criteria for employing an enzyme as an additive in detergents are: (i) it should be active at wash temperatures (20–40 °C); (ii) stable under alkaline conditions and (iii) compatible with detergents [9,11,19–24]. To estimate whether CelE1 could be used as detergent additive to improve the washing performance of the detergent, CelE1 activity was evaluated in the presence of Triton X-100 (TX) and SDS as depicted in Fig. 2. After CelE1 incubation during 15 h with 1% TX, the remaining activity was of 97% (Fig. 2A). The incubation with 15% TX during 1 and 15 h reduced slightly the CelE1 activity to 85 and 78%, respectively. At the highest TX concentration and incubation by 15 h, the CelE1 activity was reduced to 60%.

The incubation with 25 mM SDS during 1 and 3 h reduced the CelE1 activity to 94 and 81%, respectively (Fig. 2B). However, incubation with 25 mM SDS during 15 h reduced the activity to 20%. After incubation during 15 h with 1 mM SDS, the remaining CelE1 activity was of 90%. Thus, in periods of incubation lower than 3 h, both surfactants were not able to reduce the CelE1 activity significantly even at high concentrations used in our experiments. Similar behavior was observed for the endoglucanases from
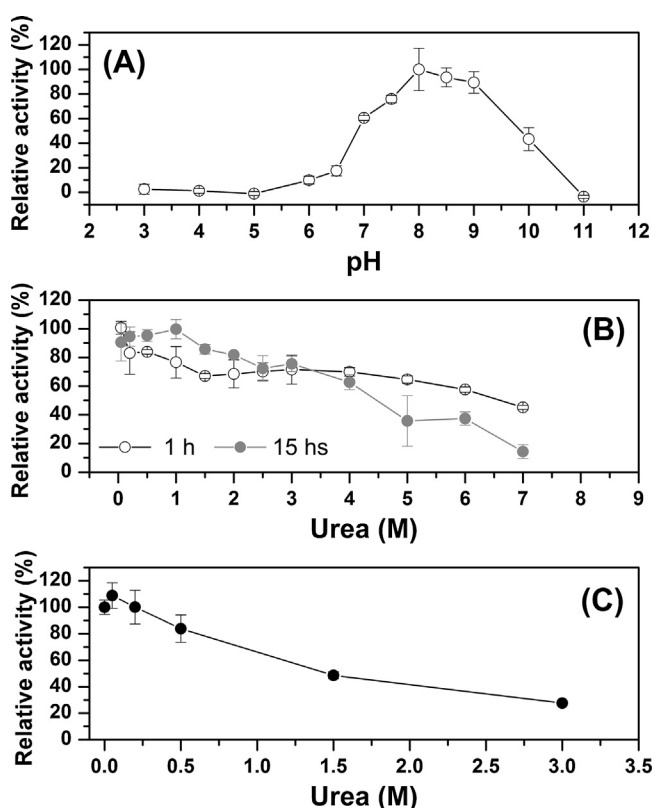

Fig. 1. Effect of pH and urea on the enzymatic activity of CelE1. (A) CelE1 relative activity at 25 °C as a function of pH (ranging from 3 to 11). (B) CelE1 relative activity at 25 °C as a function of urea concentration (ranging from 0 to 7 M). (C) Refolding of CelE1 (at 7 M urea) by dilutions against the same buffer resulting in decreasing concentrations of urea (final concentration from 3 to 0.05 M). As a control, the point at 0 M represents the relative enzyme activity in the absence of urea.
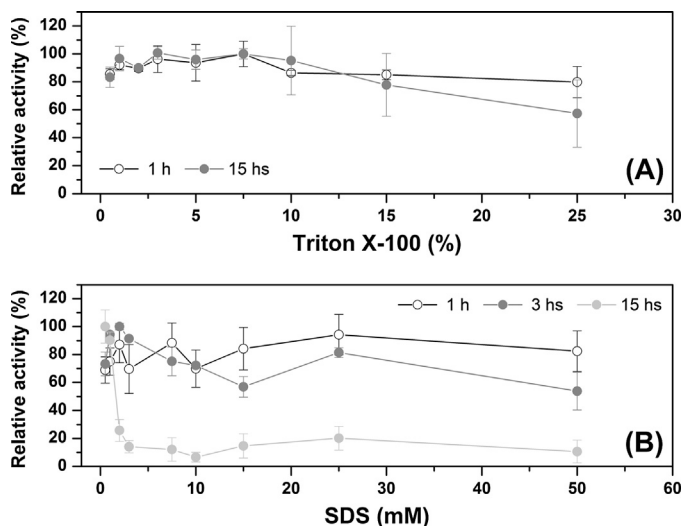

Fig. 2. Effect of surfactants on the enzymatic activity of CelE1. (A) CelE1 relative activity at 25 °C as a function of Triton X-100 concentration (ranging from 0 to 25%). (B) CelE1 relative activity at 25 °C as a function of SDS concentration (ranging from 0 to 50 mM).
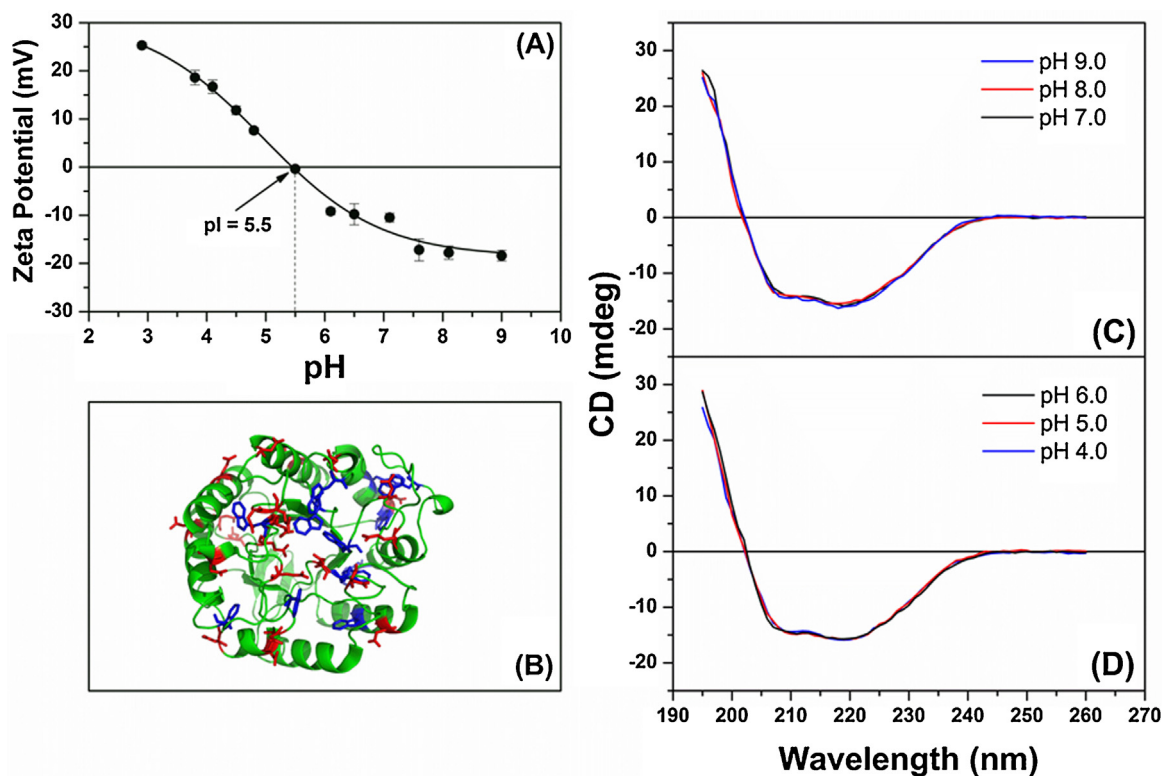
Fig. 3. Zeta-potential and circular dichroism (CD) spectroscopy. (A) Zeta-potential of CelE1 (1 mg/mL) as a function of pH at 25 °C. The black filled circles with errors bars correspond to the experimental data, and the solid line is just for the eye. (B) The crystal structure of CelE1 was recently determined at 1.8 Å resolution [8]. Schematic representation of CelE1 (PDB 4M1R) with the ionizable residues showed in red and the tryptophan residues showed in blue. The CelE1 structure has a classical $(\beta/\alpha)_8$ fold typical of members of GH5 family. CelE1 does not contain cysteine residues in its crystal structure. (C) Effect of pH on the secondary structure of CelE1 (8 μM) at 25 °C monitored by far-UV CD spectroscopy. The pH values were 9 (blue line), 8 (red line) and 7 (black line). (D) The pH values were 6 (black line), 5 (red line) and 4 (blue line). The experimental conditions are given in Section 2. (For interpretation of the references to color in this figure legend, the reader is referred to the web version of this article.)

Paenibacillus sp. IHB B 3084 (named EG5B) and *Bacillus subtilis* (named Cel5 M) when incubated with TX [19,22]. However, endoglucanase from *Paenibacillus* sp. IHB B 3084 was moderately inhibited in the presence of SDS when compared to CelE1 [19]. Furthermore, the endoglucanases from *Bacillus subtilis* [22], dairy cow rumen metagenomic library [23] and *Pseudomonas* sp. MM15 [24] were strongly inhibited in the presence of SDS.

3.4. Influence of pH on the net charge of the CelE1

In order to understand the influence of pH on the net charge, the zeta-potential of the CelE1 was determined as a function of pH (Fig. 3A). The zeta-potential of the CelE1 decreased from 25.3 ± 0.6 mV at pH 3 to -18.4 ± 1.1 mV at pH 9. The isoelectric point (pI) of CelE1 was attained at pH 5.5, condition where the zeta-potential value was close to zero [16]. The value obtained is consistent with the theoretical pI value (pI = 5.7) calculated from the amino acids sequence [13]. In addition, the experimental values of the electrophoretic mobility (μ_e) are shown in Table 1. Fig. 3B shows the crystal structure of the CelE1 with the ionizable residues in red.

3.5. Influence of pH on the structural stability of CelE1

To correlate the enzymatic activity data, described above, with the structure of the enzyme, we analyzed the influence of pH on the structural stability of CelE1 employing biophysical techniques. DLS method was used to confirm the oligomeric state of recombinant CelE1 in solution [15]. The average value of R_S was 2.6 ± 0.1 nm, even at highest protein concentration used in our experiment, which corresponds to a molecular mass of 32 ± 3 kDa

for a spherical particle. This result is consistent with a stable monomer for CelE1 in solution, whose expected molecular mass is 34 kDa (including the His tag). Furthermore, R_S of CelE1 were practically independent of pH over the range between 3 and 9 (Table 1).

Influence of pH on the secondary structure of CelE1 was studied employing CD spectroscopy. Fig. 3C and D represents the CD spectra of recombinant CelE1 measured at different pH values at 25 °C. At pH 7, CelE1 possesses a CD spectrum typical of a structure with a mixed regular secondary structure. This result is consistent with the recently determined crystal structure of CelE1 (Fig. 3B) [8]. Furthermore, the results indicated that the secondary structure of the CelE1 does not change significantly in response to decreasing the pH from 9 to 4 (Fig. 3C and D).

Table 1
Hydrodynamic radii (R_S) and electrophoretic mobility (μ_e) for CelE1 as a function of pH at 25 °C.

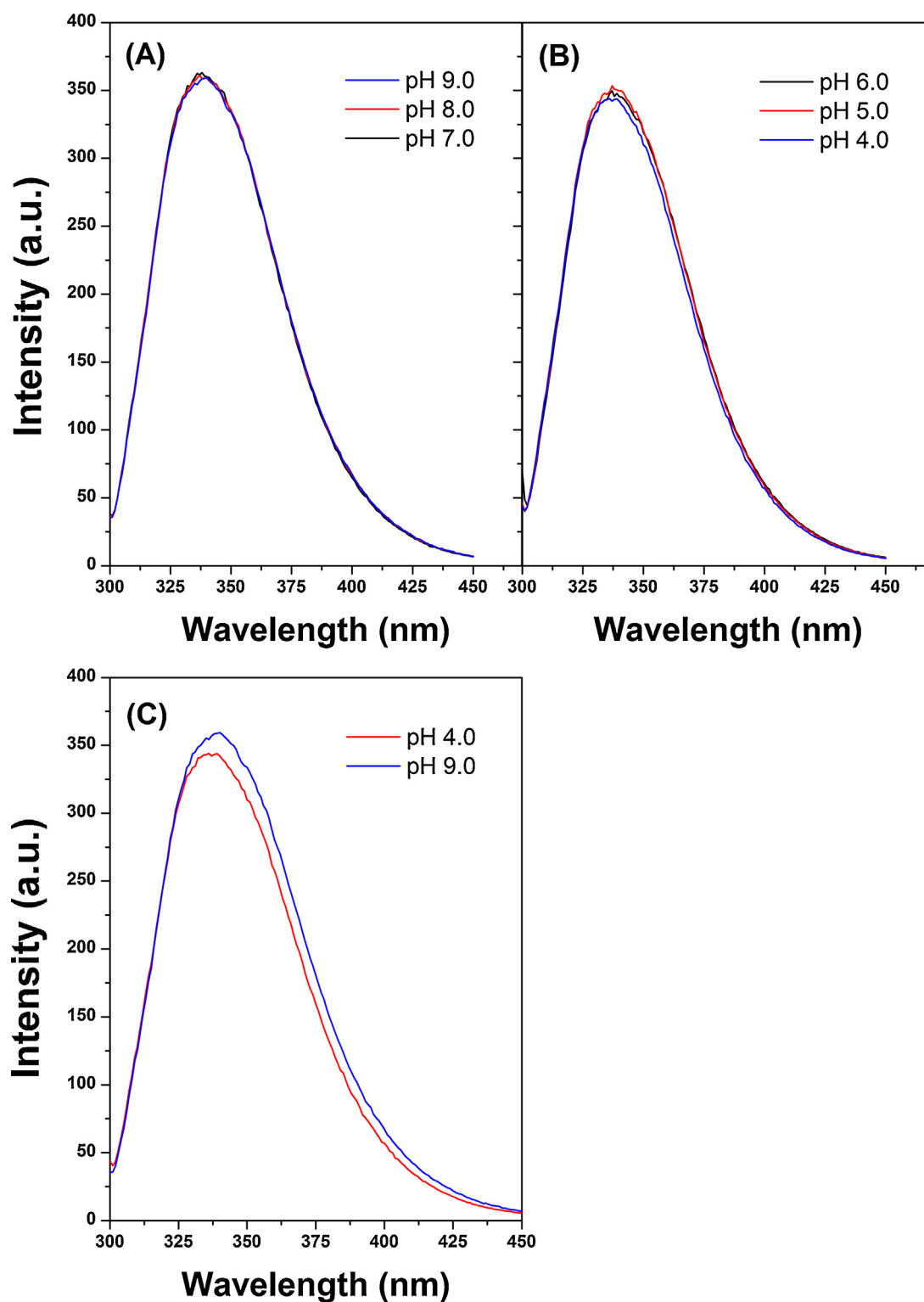| pH	Zeta-potential (mV)	μ_e [μm cm/(V s)]	R_S (nm)
3.0	25.3 ± 0.6	1.98 ± 0.04	2.7 ± 0.2
3.8	18.6 ± 1.5	1.46 ± 0.12	2.7 ± 0.1
4.1	16.7 ± 1.4	1.31 ± 0.11	2.7 ± 0.2
4.5	11.8 ± 0.9	0.92 ± 0.07	2.6 ± 0.1
4.8	7.6 ± 0.6	0.59 ± 0.04	2.6 ± 0.1
5.5	-0.4 ± 0.2	-0.03 ± 0.02	2.6 ± 0.1
6.1	-9.2 ± 0.7	-0.72 ± 0.06	2.6 ± 0.1
6.5	-9.9 ± 2.2	-0.77 ± 0.17	2.7 ± 0.1
7.1	-10.5 ± 0.9	-0.83 ± 0.08	2.6 ± 0.1
7.6	-17.2 ± 2.3	-1.35 ± 0.18	2.8 ± 0.2
8.1	-17.8 ± 1.4	-1.39 ± 0.11	2.5 ± 0.1
9.0	-18.4 ± 1.1	-1.44 ± 0.08	2.6 ± 0.1

Fig. 4. Intrinsic fluorescence spectroscopy. Effect of pH on the tertiary structure of CelE1 (3 μM) at 25 °C monitored by fluorescence spectroscopy. (A) The pH values were 9 (blue line), 8 (red line) and 7 (black line). (B) The pH values were 6 (black line), 5 (red line) and 4 (blue line). (C) Emission spectra measured at pH 9 (blue line) and 4 (red line) overlaid to make the differences between the curves. The experimental conditions are given in Section 2. (For interpretation of the references to color in this figure legend, the reader is referred to the web version of this article.)

The tertiary structure of CelE1 was analyzed by intrinsic fluorescence spectroscopy. The presence of 12 tryptophan residues in CelE1 structure (Fig. 3B) allowed us to monitor possible conformational changes induced in the enzyme. Fig. 4 shows the fluorescence emission spectra of CelE1, at several pH values, after excitation at 295 nm. The spectrum at pH 7 is characterized by a

maximum emission at 338 nm, typical of tryptophan residues, on average, partially exposed to buffer environment. Similar results were observed when CelE1 was incubated at pH 8 and 9 (Fig. 4A), indicating that there are no appreciable conformational changes induced in the enzyme and its tryptophan residues positions. However, the spectra at acidic pH conditions are characterized by a

maximum emission at 336 nm, a reduction in quantum yield of the tryptophan residues, and a blue-shift in the spectral center of mass (Fig. 4B). This result indicates that there are conformational changes induced in the protein and that the tryptophan residues are, on average, less exposed to the buffer environment. Fig. 4C shows the spectra measured at pH 9 and 4 overlaid to make the differences between the curves.

Although variation in pH showed a small effect in the enzyme structure at 25 °C (Figs. 3 and 4), the enzymatic activity was highly influenced principally at acidic conditions (Fig. 1A). The net charge determined for CelE1 (Fig. 3A) can explain the origin of the conformational changes observed by fluorescence method at acidic conditions [25,26]. Small change was observed in the net charge of the CelE1 between pH 7 (-10.5 ± 0.9 mV) and 9 (-18.4 ± 1.1 mV), in agreement with the insignificant conformational changes observed. This result is in agreement with the small variation in the enzymatic activity observed between pH 7 and 9 (Fig. 1A). However, strong change in the net charge of the CelE1 takes place between pH 7 (-10.5 ± 0.9 mV) and 4 (16.7 ± 1.4 mV). The larger positive net charge acquired at pH 4, which causes repulsion among charged groups, is likely to be responsible for the conformational changes observed. The marked variation in activity observed at pH 4 (Fig. 1A) was probably a consequence of the conformational change that becomes the active site less or more accessible to substrate when compared with the conformation at pH 8 [25,26].

3.6. Chemically induced unfolding of CelE1

In order to better understand the unfolding/refolding process of CelE1, we analyzed its chemically induced unfolding in the presence of urea monitored by biophysical techniques. Fig. 5A

shows the CD spectra of CelE1 as a function of urea concentration at pH 7 and 25 °C. The secondary structure of CelE1, monitored via the ellipticity at 220 nm, was observed to be stable up to about 2.5 M urea (Fig. 5B). However, a progressively decrease in the ellipticity at 220 nm was observed when the urea concentration was increased above 2.5 M, suggesting a loss of α-helix secondary structure in CelE1. The CD spectrum of CelE1 at 7.5 M urea is typical of a protein that has lost its secondary structure. The unfolding process of CelE1, monitored by CD method, showed a sigmoidal curve (Fig. 5B). Fitting the curve resulted in a $[U]_{1/2} = 4.5 \pm 0.1$ M, where $[U]_{1/2}$ is the urea concentration at which 50% of the enzyme exist in denatured state. Furthermore, this curve (sigmoidal-like transition) suggests that there are no detectable amounts of intermediate states present during the chemical unfolding process [17,18]. The determined value for the free energy of unfolding, considering a two-state transition, was $\Delta G^{H2O}_D = 6.4 \pm 0.2$ kcal mol^{-1} with $m = 0.85 \pm 0.02$ kcal mol^{-1} M^{-1}.

A good test to check a two-state transition is to analyze whether changes in secondary structure occur concomitantly with the changes in tertiary structure [17,18]. Again, the presence of 12 tryptophan residues in CelE1 structure (Fig. 3B) allowed us to analyze the chemically induced unfolding process by monitoring the fluorescence emission intensity at 338 nm. CelE1 in the absence of urea showed maximum emission at 338 nm, typical of tryptophan residues, on average, partially exposed to the solvent (Fig. 5C). However, the incubation of CelE1 with high urea concentrations resulted in a strong quenching of fluorescence, and an expressive bathochromic red-shift (from 338 to 352 nm) (Fig. 5C). The bathochromic red-shift observed is compatible with the tryptophan residues highly exposed to the buffer, allowing us to suppose the CelE1 completely unfolded [18]. Furthermore, the existence of an isostilbic point at 376 nm in the set of fluorescence
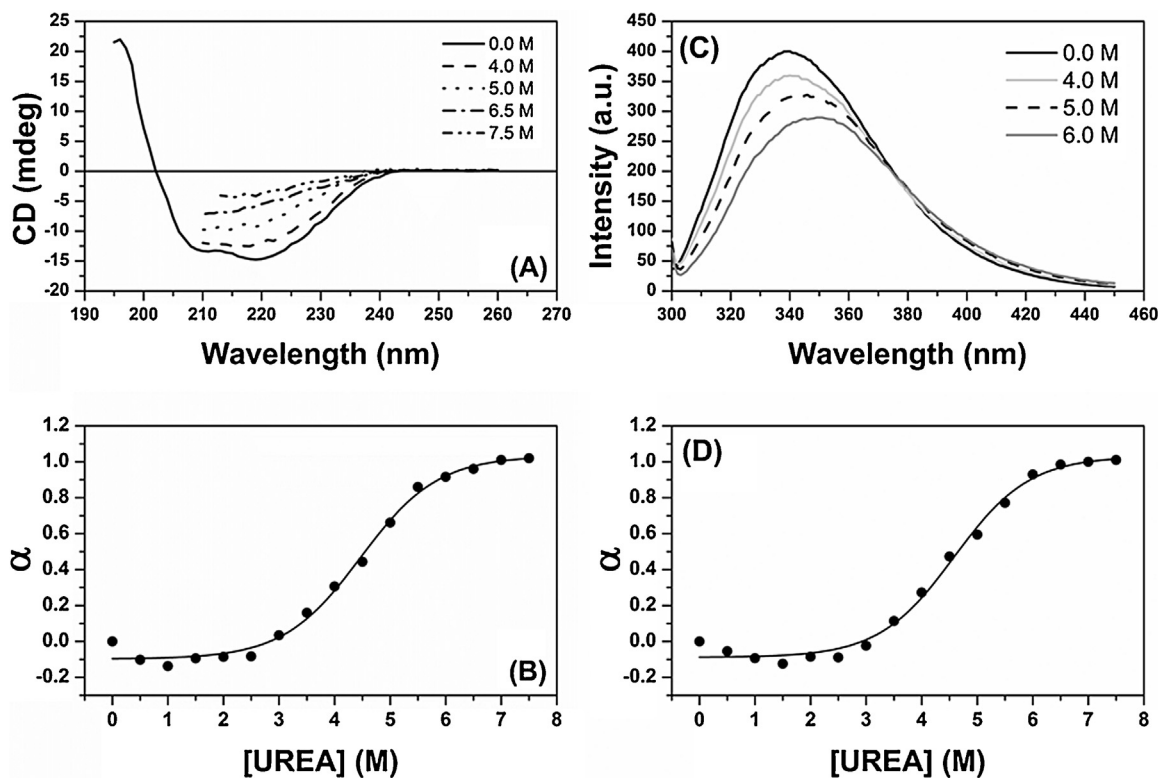

Fig. 5. Chemical unfolding monitored by CD spectroscopy and fluorescence spectroscopy. (A) Recombinant CelE1 (8 μM) was monitored by far-UV CD spectroscopy as a function of urea concentration at 25 °C. Due to the increases absorption of urea at lower wavelengths several spectra are limited due to the poor signal-to-noise ratio. (B) Ellipticity changes at 220 nm (plotted as α) as a function of urea concentration. (C) The effect of urea induced unfolding on the tertiary structure of CelE1 (3 μM) at 25 °C. (D) Fluorescence intensity at 338 nm as a function of urea concentration. The experimental conditions are given in Section 2.
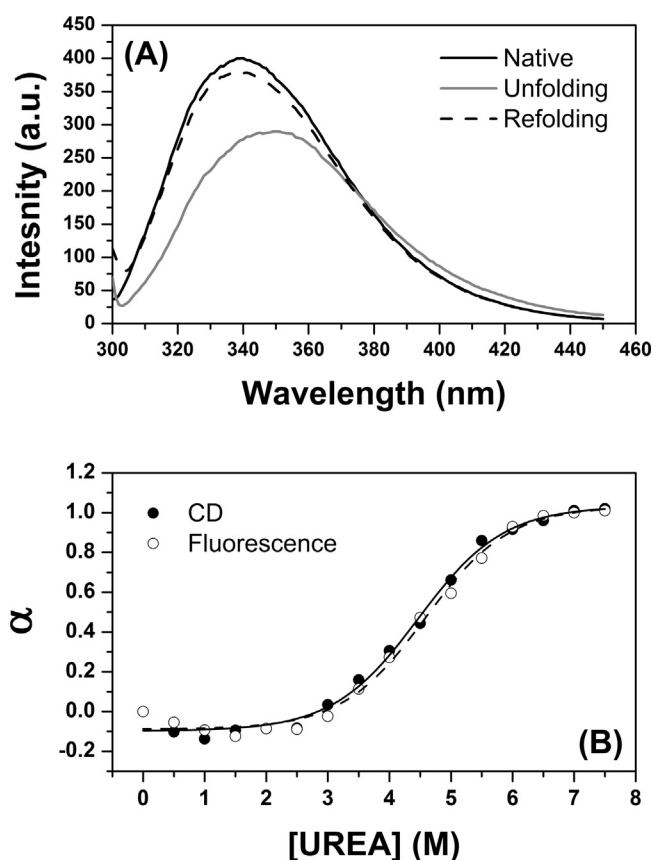
Fig. 6. Reversible chemical unfolding. (A) Fluorescence spectra of CelE1 in native, unfolded and refolded states. (B) Comparison curves of CelE1 chemical unfolding by circular dichroism (filled circles) and fluorescence (open circles).

emission spectra (Fig. 5C) is a strong evidence that the chemical unfolding of CelE1 proceeds as a two-state process [18].

The intensity fluorescence emission of CelE1 at 338 nm was monitored as a function of urea concentration (Fig. 5D). A sigmoidal transition curve was observed with a $[U]_{1/2}$ of 4.6 ± 0.1 M. Again, the curve obtained suggests that there are no intermediate states accumulated during the chemical unfolding process. The values determined for $\Delta G^{H2O}_D = 6.7 \pm 0.2$ kcal mol^{-1} e $m = 0.87 \pm 0.02$ kcal mol^{-1} M^{-1} are in good agreement, within experimental error, with the results obtained from the CD analysis described above. In addition, both curves (CD and fluorescence method) can be superimposed (Fig. 6). Thus, the data were analyzed employing a two-state model in which two populations exist at equilibrium (folded and unfolded monomers). Furthermore, the refolding of CelE1 showed that chemical unfolding by urea was a reversible process (Fig. 6A). Unfolded and subsequently refolded CelE1 maintains approximately 90% its native fluorescence emission signal in the conditions described in this study.

4. Conclusion

In conclusion, although variation in pH showed a small effect in the enzyme structure, the activity was highly influenced at acidic conditions, while reached the optimum activity at pH 8. Furthermore, the chemical unfolding/refolding of CelE1 proceeds as a reversible two-state process. Finally, surfactants were not able to reduce the CelE1 activity significantly. CelE1 showed high activity under low temperature, alkaline conditions and along with surfactants. Therefore, CelE1 was found to be promising candidate for use as detergent additives. To better estimate its potential, CelE1 will be analyzed more extensively. This study can

be useful for biotechnological applications, especially in detergent industries.

Author contributions

TVS, JNA, VMS, ACP, ML, WG: carried out the production and purification of CelE1. TVS, JNA, VMS, ACP, ML, WG: carried out the experiments. WG: coordinated the overall study, and contributed to the analysis of the results and finalizing the paper. ML, FMS, TMA, WG: suggested modifications to the draft and approved the final manuscript.

Acknowledgement

References

[1] W.H. Zyl, S.H. Rose, K. Trollope, J.F. Görgens, Fungal β-mannanases: mannan hydrolysis, heterologous production and biotechnological applications, Process Biochem. 45 (2010) 1203–1213.
[2] C.A. Rezende, M.A. Lima, P. Maziero, E.R. Deazevedo, W. Garcia, I. Polikarpov, Chemical and morphological characterization of sugarcane bagasse submitted to a delignification process for enhanced enzymatic digestibility, Biotechnol. Biofuels 4 (1) (2011) 54.
[3] B. Henrissat, G. Davies, Structural and sequence-based classification of glycoside hydrolases, Curr. Opin. Chem. Biol. 7 (5) (1997) 637–644.
[4] L.R. Lynd, P.J. Weimer, W.H. van Zyl, I.S. Pretorius, Microbial cellulose utilization: fundamentals and biotechnology, Microbiol. Mol. Biol. Rev. 66 (3) (2002) 506–577.
[5] F. Colussi, W. Garcia, F.R. Rosseto, B.L.S. Mello, M. Oliveira Neto, I. Polikarpov, Effect of pH and temperature on the global compactness, structure, and activity of cellobiohydrolase Cel7A from Trichoderma harzianum, Eur. Biophys. J. 41 (1) (2012) 89–98.
[6] A. Sørensen, M. Lübeck, P.S. Lübeck, B.K. Ahring, Fungal β-glucosidases: a bottleneck in industrial use of lignocellulosic materials, Biomolecules 3 (3) (2013) 612–631.
[7] F. Colussi, V.M. Silva, I. Miller, J. Cota, L.C. Oliveira, M. Oliveira-Neto, F.M. Squina, W. Garcia, Oligomeric state and structural stability of two hyperthermophilic β-glucosidases from Thermotoga petrophila, Amino Acids 47 (5) (2015) 937–948.
[8] T.M. Alvarez, J.H. Paiva, D.M. Ruiz, J.P.L.F. Cairo, I.O. Pereira, D.A.A. Paixão, R.F. Almeida, C.C.C. Tonoli, R. Ruller, C.R. Santos, F.M. Squina, M.T. Murakami, Structure and function of a novel celulase 5 from surgacane soil metagenome, PLoS One 8 (12) (2013) e83635.
[9] S. Ito, Alkaline cellulases from alkaliphilic Bacillus: enzymatic properties, genetics, and application to detergents, Extremophiles 1 (2) (1997) 61–66.
[10] R. Kumar, S. Singh, O.V. Singh, Bioconversion of lignocellulosic biomass: biochemical and molecular perspectives, J. Ind. Microbiol. Biotechnol. 35 (5) (2008) 377–391.
[11] R.C. Kasana, A. Gulati, Cellulases from psychrophilic microorganisms: a review, J. Basic Microbiol. 51 (6) (2011) 572–579.
[12] M.S. Showell, Enzymes, detergents, in: M.C. Flickinger, S.W. Drew (Eds.), The Encyclopedia of Bioprocess Technology, 2, Wiley, New York, 1999, pp. 958–971.
[13] E. Gasteiger, C. Hoogland, A. Gattiker, S. Duvaud, M.R. Wilkins, R.D. Appel, A. Bairoch, Protein identification and analysis tools on the ExPASy server, in: M. John Walker (Ed.), The Proteomics Protocols Handbook, Humana Press, 2005, pp. 571–607.
[14] G.L. Miller, Use of dinitrosalicylic acid reagent for determination of reducing sugar, Anal. Chem. 31 (1959) 426–428.
[15] M. Hall, J. Rubin, S.H. Behrens, A.S. Bommarius, The cellulose-binding domain of cellobiohydrolase Cel7A from Trichoderma reesei is also a thermostabilizing domain, J. Biotechnol. 155 (4) (2011) 370–376.
[16] B. Jachimska, M. Wasilewska, Z. Adamczyk, Characterization of globular protein solutions by dynamic light scattering, electrophoretic mobility, and viscosity measurements, Langmuir 24 (13) (2008) 6866–6872.
[17] A.F. Garcia, W. Garcia, M.C. Nonato, A.P. Araújo, Structural stability and reversible unfolding of recombinant porcine S100A12, Biophys. Chem. 134 (3) (2008) 246–253.

[18] M. Balsera, M. Menéndez, J.L. Sáiz, J. de Las Rivas, J.M. Andreu, J.B. Arellano, Structural stability of the PsbQ protein of higher plant photosystem II, Biochemistry 43 (44) (2004) 14171–14179.

[19] H. Dhar, R.C. Kasana, A. Gulati, Heterologous expression and characterization of detergent stable endoglucanase EG5B from Paenibacillus sp. IHB B 3084, J. Mol. Catal. B Enzym. 120 (2015) 9–15.

[20] B.Y. Chen, H.T. Wang, Utility of enzymes from *Fibrobacter succinogenes* and *Prevotella ruminicola* as detergent additives, J. Ind. Microbiol. Biotechnol. 35 (8) (2008) 923–930.

[21] S. Biver, A. Stroobants, D. Portetelle, M. Vandenbol, Two promising alkaline β-glucosidases isolated by functional metagenomics from agricultural soil, including one showing high tolerance towards harsh detergents, oxidants and glucose, J. Ind. Microbiol. Biotechnol. 41 (3) (2014) 479–488.

[22] M. Zafar, S. Ahmed, M.I.M. Khan, A. Jamil, Recombinant expression and characterization of a novel endoglucanase from Bacillus subtilis in *E. coli*, Mol. Biol. Rep. 41 (5) (2014) 3295–3302.

[23] X. Gong, R.J. Gruninger, M. Qi, L. Paterson, R.J. Forster, R.M. Teather, T.A. McAllister, Cloning and identification of novel hydrolase genes from a dairy cow rumen metagenomic library and characterization of a cellulase gene, BMC Res. Notes 5 (2012) 566–576.

[24] J. Yang, H. Dang, Cloning and characterization of a novel cold-active endoglucanase establishing a new subfamily of glycosyl hydrolase family 5 from a psychrophilic deep-sea bacterium, FEMS Microbiol. Lett. 325 (1) (2011) 71–76.

[25] S.V. Pingali, H.M. O'Neill, J. McGaughey, V.S. Urban, C.S. Rempe, L. Petridis, J.C. Smith, B.R. Evans, W.T. Heller, Small angle neutron scattering reveals pH-dependent conformational changes in *Trichoderma reesei* cellobiohydrolase I: implications for enzymatic activity, J. Biol. Chem. 286 (37) (2011) 32801–32809.

[26] L.C. Oliveira, V.M. Silva, F. Colussi, A.D. Cabral, M. Oliveira Neto, F.M. Squina, W. Garcia, Conformational changes in a hyperthermostable glycoside hydrolase: enzymatic activity is a consequence of the loop dynamics and protonation balance, PLoS One 10 (2) (2015) e0118225.